

Extended Holstein small polaron model for charge transfer in dry DNA

Yi Wang^{a,b,*}, Liang Fu^b, Ke-Lin Wang^b

^a Institute of Thin Film and Nano materials, Wuyi University, Jiangmen 529020, P.R. China

^b Department of Astronomy and Applied Physics, University of Science and Technology of China, Hefei 230026, P.R. China

Received 17 August 2005; received in revised form 13 September 2005; accepted 13 September 2005

Available online 12 October 2005

Abstract

In this paper, the charge transfer problem in dry DNA was investigated by employing an extended Holstein small polaron model with external potential traps being involved in consideration. The ground state energy and the probability amplitude of polaron in various DNA chains with different external trap potentials were obtained by variational method with the trial function being taken in coherent state form. The stability of transferred charges in various circumstances was discussed accordingly.

© 2005 Elsevier B.V. All rights reserved.

PACS: 87.15.Aa; 71.38.-k; 87.14.Gg; 72.80.Le

Keywords: Small polaron; Dry DNA; Potential trap; Coherent state

1. Introduction

Recently, the phenomenon of charge transport in DNA has attracted intense study of biologists, chemists and physicists [1–23]. Charge transfer in DNA was first put forward by Eley and Spevey in 1962 [3]. The research on DNA conductivity is of great interest as charge transfer to provide for fabricating nanoscale structures, and the charge injection can be associated with damage, mutation, and repair processes in DNA [1,2,11,12]. From the theoretical side, it was suggested that π – π interactions of stacked base pairs in double-stranded DNA could lead to conducting behavior [3]. The reason behind this idea was that DNA's bases are aromatic entities, i.e., the organic compounds containing planar, unsaturated, benzene-type ring structures, whose atomic p_z orbitals perpendicular to the plane of the base can form rather delocalized π bonding and π^* antibonding orbitals. From the experimental side, measurements on single DNA molecules have been made in recent years [4,9]. Early measurements of electron transfer in DNA were performed with a variety of techniques, and yielded apparently contrasting results. Now it has been recognized that this was partly due to the variety of DNA sequences, layouts and conditions. Taking experimental conditions for example, in

a saline solution, calculations suggest that counterions play an essential role [19,20]. In the absence of salt, mechanisms that do not involve counterions, such as bandlike electronic transport, [10], intrinsic vibrational hot spots [14–16], variable range hopping, [21] and small polaron motion [22,23], have been proposed and found to be more relevant. Among these, as a feasible candidate, the small polaron mechanism has been proposed to explain certain phenomena of charge transfer in dry DNA. In this mechanism, the polaron was considered as the bound state of the charge carrier (electron or hole) and the deformation of the DNA bases, guanine(G), cytosine(C), adenine(A) and thymine(T) [13,18,22,23].

In addition, the DNA sequence plays an important role in transport phenomena in DNA. To understand why it makes a difference, we need to compare the relative energies of the G–C and A–T base pairs. These energies have now been deduced from computational models, photoemission experiments and electrochemical measurements. The important feature is that a hole, i.e., a positive charge, is more stable on a G–C base pair than on an A–T base pair. Also, the energy difference between these two pairs is substantially larger than the thermal energy of the charge carrier. Under these conditions, a hole will localize on a particular G–C base pair. Because the A–T base pairs have a higher energy, they act as a barrier to hole transfer. However, the hole can tunnel in a coherent fashion from the first G–C site to the second, and can then either hop back to the first G–C pair or move on to the next one.

* Corresponding author. Institute of Thin Film and Nano materials, Wuyi University, Jiangmen 529020, P.R. China.

E-mail address: yiwangll@yahoo.com.cn (Y. Wang).

A serious complication in the study of DNA as an electronic material is the strong influence of molecular vibrations. Particularly, the root-mean-square vibrational displacement of a basepair in DNA at room temperature is estimated to be about 0.3–0.4 Å [24], which is a tenth of the lattice constant and an order of magnitude higher than in crystals at room temperature. In this case, we expect that the formation of polaron becomes a possible mechanism in DNA. Indeed, detailed electrical transport measurements through DNA molecules of identical base pairs have been reported recently [9]. These results fit well a model in which the conduction is due to thermal motion of small polarons. In addition, numerical calculations also report the possibility of small polarons in dry DNA [18]. However, other mechanisms may be also the candidate to explain the transport phenomenon in DNA, which will not be involved in consideration in the present paper [1,2].

The physics of polarons is that of an electron (hole), added to an otherwise empty (filled) band, and coupled to lattice deformations [25]. In the case of DNA, the electron (hole) moves in a band formed by the interbase hybridization of p_z orbitals perpendicular to the planes of the stacked base pairs in double-stranded DNA. Hence the coupling interaction between electron (hole) and molecular vibrations are usually described in small polaron regime. In this regime, the electron (hole) and lattice deformation are remarkable within a few lattice sites. Therefore the discrete nature of lattice manifests that the continuum description is inappropriate and instead calls for a discrete model.

2. Holstein small polaron model

Holstein model has been widely used as a starting point for the study of small polarons [18,25]. The extended Hamiltonian of Hostein polaron model can be given by

$$H = -t \sum_j \left[\left(C_j^\dagger C_{j+1} + H.c. \right) \right] - g \sum_j C_j^\dagger C_j X_j + \sum_j \left(\frac{P_j^2}{2m} + \frac{1}{2} K X_j^2 \right) \quad (1)$$

where the first term is a tight-binding expression which is used to describe the electronic hopping between adjacent base pairs, and t is the hopping constant (or transfer integral). C (C^\dagger) is the annihilation (creation) operator of the charge. The second term describes an on-site charge-lattice coupling between a geometric displacement X_j and the electron (hole) presence at site j , and g the charge-lattice coupling strength. The last term in Eq. (1) represents the sum of kinetic energy and potential energy of the lattice.

Since the biological DNA is an intrinsically non-periodic structure, four bases have different ionization potentials. Thus, if one removes an electron from the chain, the resulting hole may feel the on-site potentials $V_{CG} < V_{AT}$. Therefore the sequence of DNA base pairs determines the potential profile

of the chain. This motivates us to add an external potential term to the Hamiltonian (1) and yields

$$H = \sum_j V_j C_j^\dagger C_j - t \sum_j \left[\left(C_j^\dagger C_{j+1} + H.c. \right) \right] - g \sum_j C_j^\dagger C_j X_j + \sum_j \left(\frac{P_j^2}{2m} + \frac{1}{2} K X_j^2 \right) \quad (2)$$

where $V_j < 0$ is the external ionization potential of DNA sequence located at j -th sit. By introducing a transformation to express the displacement X and the momentum P in terms of phonon creation and annihilation operators

$$X_j = \sqrt{\frac{\hbar}{2m\omega}} (a_j + a_j^\dagger), \quad P_j = i\sqrt{\frac{\hbar m\omega}{2}} (a_j - a_j^\dagger), \quad (3)$$

where $\omega = \sqrt{\frac{K}{m}}$, a_j and a_j^\dagger are the annihilation and creation operator obeying bosonic commutation relation $[a_i, a_j^\dagger] = \delta_{ij}$. The Hamiltonian (1) can then be recast into

$$H = \sum_j \left[V_j C_j^\dagger C_j - t \left(C_j^\dagger C_{j+1} + H.c. \right) \right] - g \sqrt{\frac{\hbar}{2m\omega}} \sum_j C_j^\dagger C_j (a_j + a_j^\dagger) + \sum_j \hbar\omega a_j^\dagger a_j \quad (4)$$

To investigate the ground state property, we employ the variational method by adopting the following trial function form

$$|\Psi\rangle_g = \left(\sum_j \Psi_j C_j^\dagger \right) \times e^{\sum_j \left(-\frac{\alpha_j^2}{2} + \alpha_j a_j^\dagger \right)} |0\rangle. \quad (5)$$

It is noticed that the phonon part of the trial function is in the form of coherent state. The reason of this choice is as follows: (1) We had employed the coherent state as the trial wave function of polaron to describe the electron–phonon interaction, and many interesting remarkable results had been obtained [26]; (2) One author of this paper had calculated the band structure of Holstein model with coherent state for the phonon part and the results are in good agreement with the numerical calculation [27,28]; (3) In the Jaynes–Cummings model of quantum optics, if the case is near resonant, the Boson part takes the state function as Fock state, and if the case is far away from resonant, then it takes the form of coherent state. Since there exist many different modes of phonon in Holstein model and they are mostly not in the near resonant case. Thus we take the trial wave function with the form of coherent state. Combining Eqs. (4) and (5), we have

$$E[\{\Psi_j\}, \{\alpha_j\}] = {}_g\langle \Psi | H | \Psi \rangle_g = \left(\sum_j z \hbar \omega \alpha_j^2 \right) \left(\sum_k \Psi_k^2 \right) + \sum_j \left(V_j \Psi_j^2 + 2t \Psi_j \Psi_{j+1} \right) + g \sqrt{\frac{2\hbar}{m\omega}} \sum_j \Psi_j^2 \alpha_j \quad (6)$$

Minimizing $E[\Psi_j, \alpha_j]$ with respect to α_j and Ψ_j under the normalization condition $\sum_j \Psi_j^2 = 1$, we obtain

$$\alpha_j = -\frac{1}{\sqrt{2m\hbar\omega^3}} g \Psi_j^2, \quad (7)$$

and

$$\Psi_j \left(\sum_k \hbar\omega\alpha_k^2 \right) + V_j \Psi_j - t(\Psi_{j+1} + \Psi_{j-1}) - g\sqrt{\frac{2\hbar}{m\omega}} \Psi_j \alpha_j - E \Psi_j = 0, \quad (8)$$

where E is the Lagrange multiplier taking care of the normalization condition, and the ground state energy of the system. Substituting Eq. (7) into Eq. (8), we get

$$\left(E - V_j - \sum_k \frac{g^2 \Psi_k^4}{2m\omega^2} \right) \Psi_j = -t(\Psi_{j+1} + \Psi_{j-1}) - \frac{g^2}{m\omega^2} \Psi_j^3. \quad (9)$$

and further

$$E[\{\Psi_j\}] = \sum_j \left(V_j \Psi_j^2 - t(\Psi_{j+1} \Psi_j + \Psi_j \Psi_{j-1}) - \frac{g^2}{2K} \sum_j \Psi_j^4 \right). \quad (10)$$

Based on Eq. (10), we will have a better understanding of small polaron formed by self-trapping potential. First we investigate the usual situation where the V_j is uniform and set to zero. Apart from the nonlinear term $-\frac{g^2}{K} \sum_j \Psi_j^4$, the Hamiltonian describes the motion of an electron in a uniform background in the tight-binding approximation. The wave function will be extended, and sinusoid. It is precisely the last term that makes the formation of localized polaron possible. To see a transparent physics picture, we can make a self-consistent field study, i.e., to average $-\frac{g^2}{K} \sum_j \Psi_j^4$ as $-\frac{g^2}{K} \sum_j V_j^2 \Psi_j^2$, assuming that V_j^s is known. Then the Hamiltonian describes the motion of an electron in an effective external potential background $-V_j^s$. The solution Ψ_j is required to produce this effective potential self-consistently, i.e., $\Psi_j^2 = V_j^s$. The small polaron solution of the simplified Hamiltonian corresponds to the case where self-induced effective potential background is a localized potential well. If the well is deep enough, the lowest energy state is a bound state localized in the well and decay exponentially to infinity. Since the wave function has dominant amplitude in the well, the self-induced effective potential $-V_j^s = -\Psi_j^2$ turns out to be a well, in consistent with the demand. This phenomena of electron being localized in a potential well which is produced by itself is called self-trapping. Here it is mathematically described by the nonlinear term Ψ_j^4 . We recall that this nonlinear term has its origin in the lattice's degree of freedom, which means that polaron is induced by phonon–electron coupling. What's more, this picture hints that polaron cannot be formed if the phonon–electron coupling constant g is too small, or when the ion is too inert (K is too large), since in that case the self-induced effective potential well is

too weak to accommodate bound state. This picture also predicts that the energy of the polaron will decrease as the phonon–electron coupling increases, due to the increasingly deep self-induced potential trap. Finally, this picture gives us insight into the case where the true external potential background V_j is nonuniform. For example, in the case where the distribution V_j is a potential well, two cases may arise: (1) if the self-induced effective potential is a well residing at the same position as the original external potential well, the total effect is that the well is deepened, and localization effect enhanced; (2) if the self-induced effective potential is in a different place, the total effect is that the electron 'sees' two potential well. Therefore it is expected that the state in case (1) is stable and has lower energy than that of case (2). In summary, this picture of polaron formation by self-induced potential trap will guide us in the following analysis.

3. Stability analysis

Suppose that the potential $V(x)$ (either the external potential or the self-trapping effective potential) consists of two different potential wells, and for each well there is a stationary state with the wave function localized around the well. The deeper of these two states represents the ground state of the system, the shallower one is an excited state. However, the excited state may correspond either a local minimum or an unstable stationary point (saddle point). If the dynamics of the system is governed only by the equations of motion considered above, the system can remain in the excited state forever. However, if one includes fluctuations and dissipation, the character of the excited state becomes very important. For a local minimum small perturbations will not drive the system out of the vicinity of the stationary point, i.e., the particle stays in the shallow well, while in the case of an unstable point dissipation may make the system fall into the global minimum, i.e., the particle moves to the deep well. Thus, we are motivated to study whether a stationary point of the energy functional (10) is stable or not.

To analyze the stability problem, the standard treatment is to expand $E[\{\Psi_i\}]$ to second order around the stationary point. If the corresponding matrix of second order derivatives is positive (negative), the stationary point is a local minimum (maximum); if it is nonpositive, the stationary point is a saddle point. However, the procedure is plagued by the fact that $\Psi_{i,j} = 1, \dots, N$ are not independent variables, but subject to the normalization condition. Viewed geometrically, the points Ψ_i are in a N -dimensional unit spherical surface. We expand $E[\{\Psi_i\}]$ around the stationary point Ψ_i^0 ,

$$E[\Psi] = E[\Psi^0] + (\nabla E)^T|_0 (\Psi - \Psi^0) + \frac{1}{2} (\Psi - \Psi^0)^T \times \left(\frac{\partial^2 E}{\partial \Psi_i \partial \Psi_j} \right)|_0 (\Psi - \Psi^0). \quad (11)$$

We introduce an arbitrary vector $\delta\Psi$ tangential to the spherical surface at the stationary point. The vector resides

in a N-1 dimensional tangent space, i.e., $\delta\Psi \cdot \Psi^0 = 0$. Along the direction of this vector, close to the stationary point, we have

$$\Psi = \Psi^0 \left(1 - \frac{1}{2} \delta\Psi^2 \right) + \delta\Psi \quad (12)$$

to second order in $\delta\Psi$. Now the energy functional can be approximated to second order in $\delta\Psi$

$$E[\Psi] = E[\Psi^0] + (\nabla E)^T|_0 \cdot \left(\delta\Psi - \frac{1}{2} \delta\Psi^2 \Psi^0 \right) + \frac{1}{2} \delta\Psi^T \cdot \left(\frac{\partial^2 E}{\partial \Psi_i \partial \Psi_j} \right) |_0 \cdot \delta\Psi. \quad (13)$$

In the stationary point, $\nabla E|_0 = 2 E\Psi^0$ (E is the Lagrange multiplier, or the ground state energy here), therefore we have

$$E[\Psi] = E[\Psi^0] + \delta\Psi^T \left(\frac{1}{2} \frac{\partial^2 E}{\partial \Psi_i \partial \Psi_j} - E1 \right) |_0 \delta\Psi, \quad (14)$$

where 1 is identity matrix of dimension N. In the last step, we have used the orthogonality relation between $\delta\Psi$ and Ψ , as well as the normalization condition on Ψ . Now we have reduced the stability analysis to a mathematical problem: for arbitrary vector $\delta\Psi \perp \Psi$, we demand $\delta\Psi^T H \delta\Psi > 0$, where $H = \left(\frac{1}{2} \frac{\partial^2 E}{\partial \Psi_i \partial \Psi_j} - E1 \right) |_0$. It is not difficult to see that this condition is equivalent to the equations

$$H \cdot \delta\Psi = e \delta\Psi + \lambda \Psi, \quad \lambda \text{ is arbitrary} \quad (15)$$

$$\delta\Psi \cdot \Psi = 0 \quad (16)$$

permit N-1 solution $\{e_i, \delta\Psi_i\}$ and all $e_i > 0$. Equivalently, we can derive an equation for e without reference to $\delta\Psi$

$$\Psi(H - E1)^{-1} \Psi = 0. \quad (17)$$

In practice, the inverse of a big matrix with unknown parameter cannot be obtained. One way to circumvent this difficulty is to plot the linear hypersphere space of Eq. (17) for a sequence of E , and see where it approaches zero. This procedure is bothersome, and due to the existence of inverse operation, there are diverging points and hence complicates the determination of the zero points. We find that Eq. (17) can be further simplified to give a more useful and implementable expression. First, we note that

$$H_{ij} = \delta_{ij} \left(V_i - 3 \frac{g^2}{K} \Psi_i^2 \right) + \delta_{i+1,j}(-t) + \delta_{i,j+1}(-t) \quad (18)$$

is a highly sparse big matrix, with only its diagonal and nearest non-diagonal elements nonzero. In practice, the eigenvalues and eigenvectors of H up to 40×40 (the base sites up to 40) can be numerically obtained with negligible computing time. Suppose H has eigenvalues $\{h_i\}$ and corresponding normalized

eigenvectors $\{v_i\}$, then we can diagonalize H with an orthogonal matrix U , such that

$$U_{ij} = (v_j)_i, \quad (19)$$

$$H = U \cdot (h_i \delta_{ij}) \cdot U^T. \quad (20)$$

Substituting Eq. (20) into Eq. (17), we have

$$\begin{aligned} 0 &= \Psi(H - E1)^{-1} \Psi = \Psi(U \cdot (h_i - y_i) \delta_{ij} \cdot U^T)^{-1} \Psi \\ &= \Psi \left(U \cdot \frac{1}{h_i - y} \delta_{ij} \cdot U^T \right) \Psi \\ &= (U^T \Psi) \cdot \left(\frac{1}{h_i - y} \delta_{ij} \right) \cdot (U^T \Psi) = \sum_i \frac{u_i^2}{h_i - y} \equiv f(y), \end{aligned} \quad (21)$$

where u_i is the i -th component of vector $U^T \Psi$, which can be easily obtained numerically. Up to now, the structure of l.h.s of Eq. (17) is quite clear. Moreover, we can derive some useful results. For example, if all eigenvalues h_i of H are positive, the solution e of Eq. (17) cannot be negative (or else $f(y) = \sum_i \frac{u_i^2}{h_i - y} > 0$), which means the stationary point is a local minimum and the corresponding state is stable. For another example, if H has more than one negative eigenvalues, and both appear in the sum of $f(y)$, Eq. (17) must have a negative solution y between two adjacent negative eigenvalues $h_1 < y < h_2$, because as $y \rightarrow h_1^+$, $f(y)$ approaches negative infinity; as $y \rightarrow h_2^-$, $f(y)$ approaches positive infinity, and hence by continuity, there must be a y between h_1 and h_2 where $f(y) = 0$, i.e., there must be a negative solution of Eq. (17). In this case, the stationary point is a saddle point and the corresponding state is unstable. Therefore, what is worth further study is the case where H has only one negative eigenvalue.

4. Results and discussions

In what follows, we will calculate the ground state energy and the wave function of polarons in different potential distribution. Eq. (8) is a set of nonlinear equations, they can only be solved numerically. Here, it was solved by an iteration method: Given a set of initial value of $\{\Psi_j\}$ and E , the set of Eq. (8) and Eq. (10) can be used to generate new values. The process can be continued until the energy does not change. Usually the choice of initial values corresponds to physical considerations. Since we are interested in localized state, we choose the wave function at localized point almost 1, and almost 0 at all other points. It has been verified that in most cases the localized state is independent of these particular initial values. In practice, the procedure is carried out in Mathematica.

4.1. Small polaron in an uniform DNA chain

First, we consider a DNA chain consisting of the base sequence of $\cdots \text{ATGCATGCATGC} \cdots$. In this situation, the wave

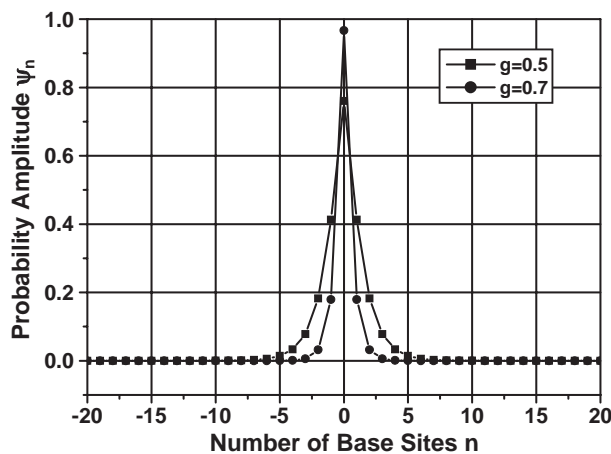


Fig. 1. The probability amplitude Ψ_n of the charge carriers as the function of DNA base sites under two different charge-lattice coupling strength. Where $t=0.1$ eV, spring constant $K=0.85$ eV/cm, lattice points $n=41$.

function which is in narrow peak form, if there is any, is wholly due to self-trapping.

The wave function of the typical electronic part of small polaron states as the function of the number of base pairing sites is plotted in Fig. 1. It is noticed that the width of the probability amplitude decreases, or the peak becomes sharper, as the phonon–electron coupling increases. In addition, we studied the stability of these states, and we found that the small polaron states will not be stable unless the charge-lattice coupling constants $g > 0.55$. That is to say there exists a critical value of charge-lattice coupling strength which corresponds to the stable polaron state that could be formed accordingly.

The profile of total polaron energy vs. charge-lattice coupling constant g is plotted in Fig. 2, illustrating that they are in a nonlinear relation. It was also told that as the phonon–electron coupling grows, the polaron has lower energy, in agreement with our previous expectation. In particular, the system does not possess bound state when charge-lattice coupling constant $g < 0.4$, because in that case, the effective potential trap is not deep enough to form bound state, in agreement with Heisenberg uncertainty principle.

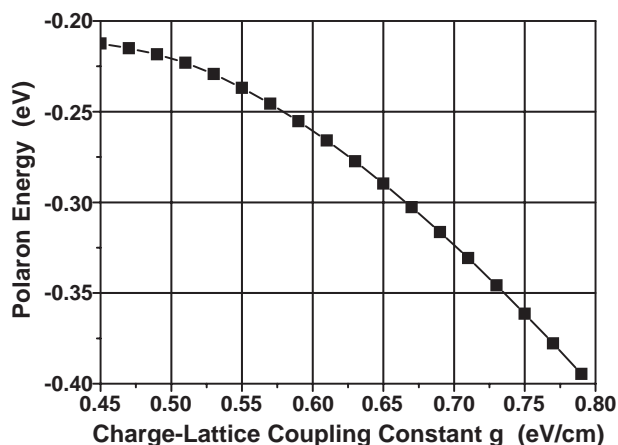


Fig. 2. The total energy of the charge carriers as a function of charge-lattice coupling strength g . Where $t=0.1$ eV, $K=0.85$ eV/cm, $n=41$.

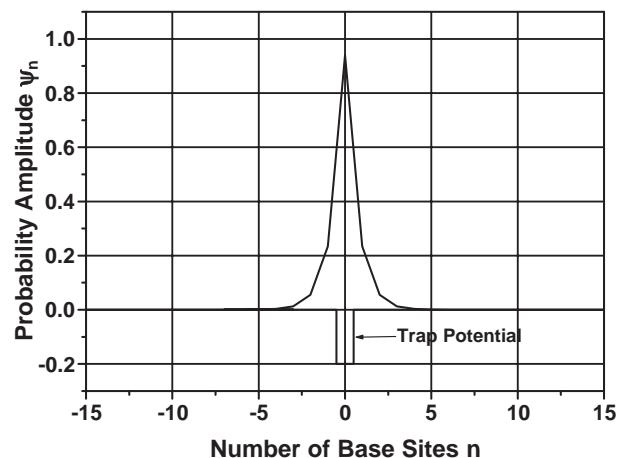


Fig. 3. Polaron probability amplitude as the function of DNA base sites in a single trap potential well $V_t=0.2$ eV with parameters $t=0.1$ eV, $K=0.85$, $g=0.4$.

4.2. Small polaron in one potential trap

Secondly we consider a single guanine on a chain consisting only of adenines acts as a trap since $V_G < V_A$ (AAAA-GAAAA). There are two kinds of states here. One is small polaron localized in the external potential trap; another is small polaron localized outside the potential trap. In the first case, the external potential trap is deepened by self-trapping. Typical electronic part of small polaron states wave function is shown in Fig. 3. Moreover, we find that as a result of the deepening effect, the critical value of the external trap V to form polaron will become smaller when phonon–electron coupling strength becomes stronger. The ground state energy vs. potential depth and phonon–electron coupling strength is shown in Fig. 4. We note from Fig. 4 that as the phonon–electron coupling strength increases, smaller V is required.

In the second case, the polaron is localized in the self-induced trap rather than an external trap elsewhere. We find that such a state can be formed and can be stabilized when phonon–electron coupling strength g is large enough, which leads to deep self-induced effective potential trap. Typical wave function of this case is shown in Fig. 5. In order to determine the stability of this

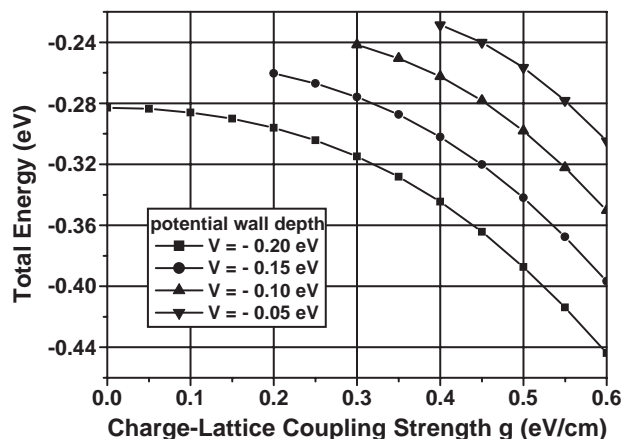


Fig. 4. Total energy as a function of charge-lattice coupling strength with different-depth potential traps.

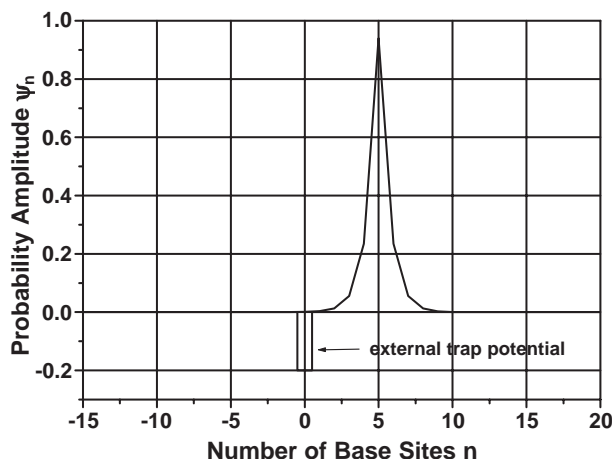


Fig. 5. A polaron can be formed outside a potential trap $V=0.2$ eV when charge-lattice coupling strength reaches $g=0.65$. The peak of the wave function is 5 bases away from the trap.

state, we plot the l.h.s. of Eq. (17) in Fig. 6, and find that Eq. (17) has no negative solution, which means the state is stable. Moreover, we find that the critical value of g not only depend on the external potential trap, but also on the distance from that trap. This distant dependence can be understood as follows: the trap acts a perturbation on the small polaron formed away from it, the farther away it is, the less the perturbation will be, and hence the more likely the polaron will be formed and stabilized. The critical value of g vs. potential depth and distance from the external trap is plotted in Fig. 7. From Fig. 7, we find that the critical value of g does not change appreciably soon after the peak is 3–4 bases away from the potential trap.

4.3. Small polaron in symmetric and asymmetric two potential traps

In third part of the article, we consider the case of two separated guanines on a DNA chain consisting of adenines represent two symmetric potential traps (such as AAAGA-GAAA, etc.). The wave function of two traps system as the

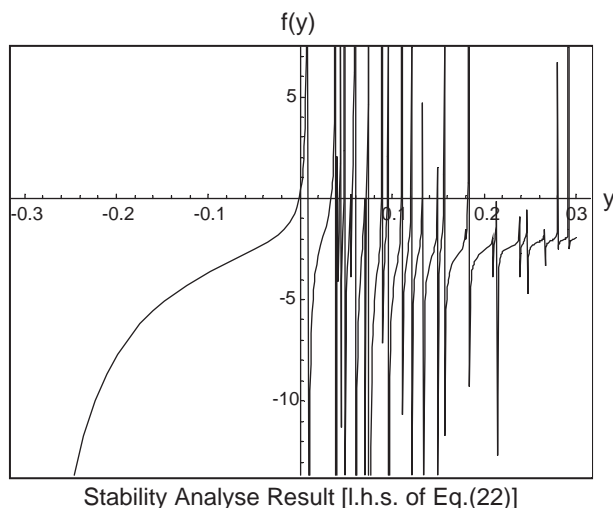


Fig. 6. Stability analysis of the polaron state in Fig. 5. None of the zeros of l.h.s. of Eq. (17) is negative, which means the state is stable.

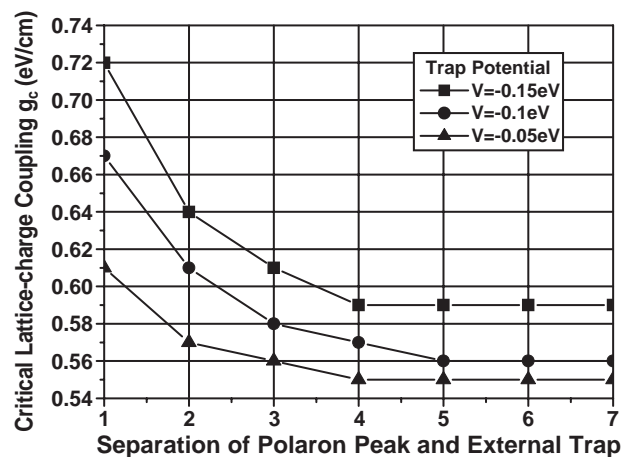


Fig. 7. Critical g values vary with the potential depth and the distance from the external trap. Where $t=0.1$ eV, $n=41$.

function of DNA pair sites are plotted in Fig. 8. We find that the symmetric double peaked wave function is not necessarily lower in energy than the single peaked state localized in either trap, in contrast to the case without phonon–electron coupling where the ground state is always the symmetric double peaked. This is because the self-trapping effect will be stronger in one trap than equally divided in two traps.

By varying the separation of two traps, we find that, for certain parameters, as plotted in Fig. 9, the ground state is double peaked when two traps are very near, and it will change to single-peaked as two traps are separated farther. The appearing of double-peak in two closer traps is mainly due to the perturbation (or the overlap of two separate polaron wave functions being located in each isolate trap) of one potential trap on the other trap. As the traps are far apart, the perturbation becomes negligible, and hence a single-peaked state persists. That also explains the fact why this phenomena only occurs for large hopping term.

Finally we consider two separated guanines of different length on a chain consisting of adenines represent two asymmetric potential traps (such as AAAGAGGAAA). In this case, two kinds of polaron localized in the shorter and longer

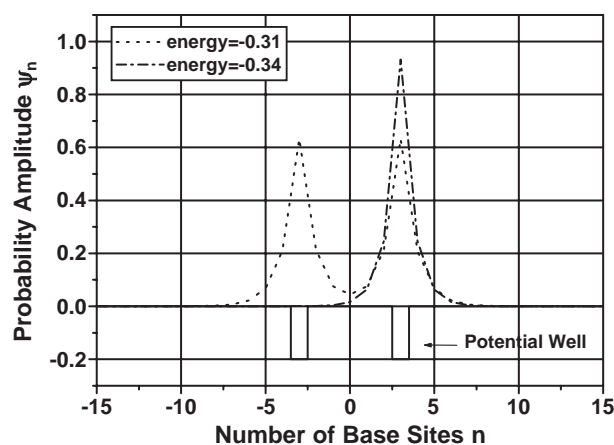


Fig. 8. Double and single peaked states in a two traps system with separation $l=7$ and parameters $g=0.4$, $V_1=V_2=-0.2$ eV. The single peaked state is lower in energy, contrary to the case without charge-lattice coupling.

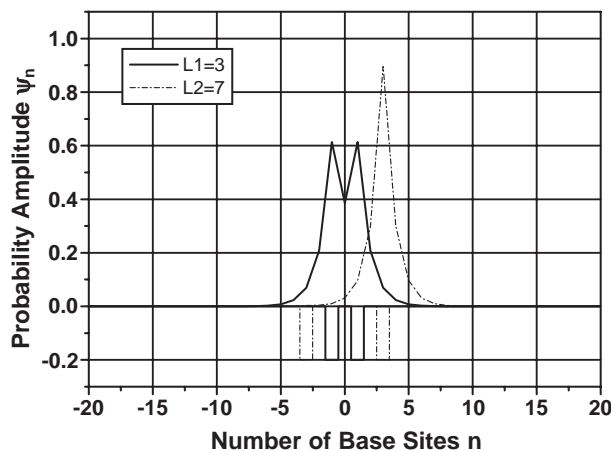


Fig. 9. Two ground state wave functions under different trap separations $l=3$ and $l=7$ with parameters $g=0.4$, $V_1=V_2=-0.4$ eV, and $t=0.2$ eV. The ground state is double peaked when $l=3$, whereas it is single peaked when $l=7$.

trap are possible. The polaron in the longer trap has a lower energy and is in ground state, while the polaron in the shorter trap is in excited state. Typical wave functions of the electronic part of these polarons and their energies are plotted in Fig. 10.

We are also interested in the stability problem of the excited state. If the state is unstable, the polaron will transfer from a shorter trap to a longer one under small perturbation. We find that as the charge-lattice coupling strength increases to a certain value (we call it a critical value), the excited state will become stable. More interestingly, we find that: (1) the value of charge-lattice coupling strength g does not change appreciably with the separation of potential traps when separated by more than 3 bases, as in the case of a single trap where polaron stays away from it; (2) such a value increases as the longer trap increases its length. The critical value of g for different trap separation and different longer trap is shown in Fig. 11.

5. Conclusion

In summary, as a possible candidate mechanism for charge transfer in dry DNA, the small polaron formation in a DNA

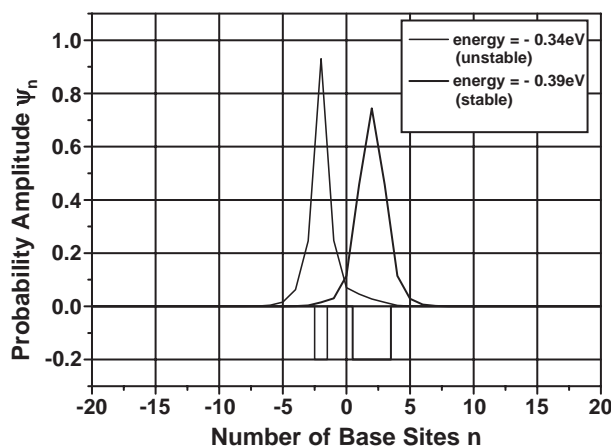


Fig. 10. Two type polarons in a molecular chain with different trap width. Where $g=0.4$, $V_1=V_2=-0.2$ eV, located at site-2 and 1,2,3, respectively. $t=0.1$ eV, $n=41$.

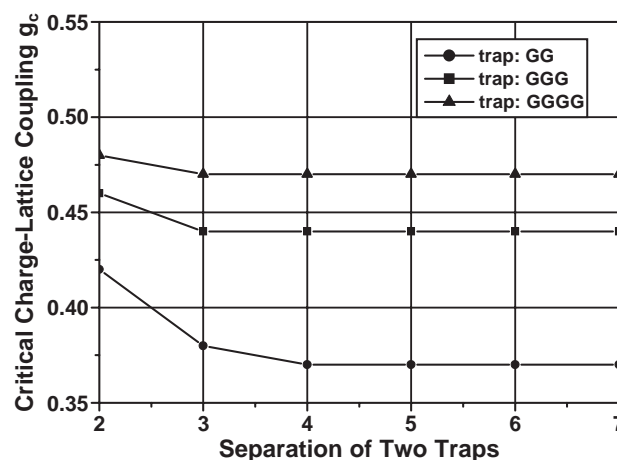


Fig. 11. Critical charge-lattice coupling values versus the separation of two external traps with parameters $t=0.1$ eV, $n=41$.

chain was studied by variational method based on extended Holstein model. The theory takes the advantage of coherent state to incorporate the motion of charge in DNA bases. The ground state energy and the wave functions of the system in various DNA chains were discussed and calculated under different external trap potentials which are corresponding to different DNA base sequences. The influence of symmetrical and asymmetrical potential traps due to the inherent molecular structure of DNA was discussed. We found that: (i) the symmetric double peaked wave function was not necessarily lower in energy than the single peaked state localized in either trap. This result is in contrast to the case without phonon–electron coupling where the ground state is always the symmetric double peaked; (ii) the appearing of double-peak in two closer traps is due to the overlap of two separate polaron wave functions being located in each isolate trap; (iii) the polaron in the longer trap has a lower ground-state energy than that of the polaron in the shorter trap. We also found that the value of charge-lattice coupling strength g does not change appreciably with the separation of potential traps when separated by more than 3 bases, but it increases with the increase of trap length. The state stability of transferred charges in DNA chain was discussed accordingly. More extensive work which link the theoretical models to the experiments requires our further investigation in the near future.

Acknowledgments

This research was supported by the Natural Science Foundation of China (granted No.50272063) and Elitist Foundation of Anhui Province (granted No. 2001Z016).

References

- [1] C. Dekker, M.A. Ratner, Electronic properties of DNA, *Phys. World* 14 (2001) 29–33.
- [2] K. Daphne, A. Romer Rudolf, A. Matthew, Turner, Electronic Transport in DNA, arXiv:q-bio. GN/0504004, (2005) and references therein.
- [3] D.D. Eley, D.I. Spivey, Coherent tunneling, *Trans. Faraday Soc.* 58 (1962) 411–415.

- [4] S.O. Kelley, J.K. Barton, Electron. transfer between bases in double helical DNA, *Science* 283 (1999) 375–381.
- [5] H.W. Fink, C. Schonenberger, Electrical conduction through DNA molecules, *Nature (Lond.)* 398 (1999) 407–410.
- [6] D. Porath, A. Bezryadin, S. Vries, C. Dekker, Direct measurement of electrical transport through DNA molecules, *Nature (Lond.)* 403 (2000) 635–638.
- [7] P. Tran, B. Alavi, G. Gruner, Charge transport along the lambda-DNA double helix, *Phys. Rev. Lett.* 85 (2000) 1564–1567.
- [8] P.J. de Pablo, F. Moreno-Herrero, J. Colchero, et al., Absence of dc-conductivity in lambda-DNA, *Phys. Rev. Lett.* 85 (2000) 4992–4995.
- [9] K.H. Yoo, D.H. Ha, J.-O. Lee, et al., Electrical conduction through poly(dA)-poly(dT) and poly(dG)-poly(dC) DNA molecules, *Phys. Rev. Lett.* 87 (4) (2001) 198102.
- [10] G. Cuniberti, L. Craco, D. Porath, C. Dekker, Backbone-induced semiconducting behavior in short DNA wires, *Phys. Rev. B* 65 (4) (2002) 241314.
- [11] T. Heim, T. Melin, D. Deresmes, D. Vuillaume, Localization and delocalization of charges injected in DNA, *Appl. Phys. Lett.* 85 (2004) 2637–2639.
- [12] Hao Wang, James P. Lewis, F. Sankey Otto, Band-gap tunneling states in DNA, *Phys. Rev. Lett.* 93 (4) (2004) 016401.
- [13] R.G. Endres, D.L. Cox, R.R.P. Singh, The quest for high-conductance DNA, *Rev. Mod. Phys.* 76 (2004) 195–215.
- [14] S. Komineas, G. Kalsakas, A.R. Bishop, Effects of intrinsic base-pair fluctuations on charge transport in DNA, *Phys. Rev. E* 65 (4) (2002) 061905.
- [15] G. Kalosakas, K.Φ. Rasmussen, A.R. Bishop, Charge trapping in DNA due to intrinsic vibrational hot spots, *J. Chem. Phys.* 118 (2003) 3731–3735.
- [16] P. Maniadiis, G. Kalosakas, K.Φ. Rasmussen, A.R. Bishop, Polaron normal modes in the Peyrard–Bishop–Holstein model, *Phys. Rev. B* 68 (11) (2003) 174304.
- [17] Tadao Takada, Kiyohiko Kawai, Mamoru Fujitsuka, Tetsuro Majima, Direct observation of hole transfer through double-helical DNA over 100 \AA , *PNAS* 101 (2004) 14002–14006.
- [18] S.S. Alexandre, E. Artacho, J.M. Soler, H. Chacham, Small polarons in dry DNA, *Phys. Rev. Lett.* 91 (4) (2003) 108105.
- [19] R.N. Barnett, C.L. Cleveland, A. Joy, U. Landman, G.B. Schuster, Charge migration in DNA: ion-gated transport, *Science* 294 (2001) 567–571.
- [20] F.L. Gervasio, P. Carloni, M. Parrinello, Electronic structure of wet DNA, *Phys. Rev. Lett.* 89 (4) (2002) 108102.
- [21] Z.G. Yu, X. Song, Variable range hopping and electrical conductivity along the DNA double helix, *Phys. Rev. Lett.* 86 (2001) 6018–6021.
- [22] R. Bruinsma, G. Gruner, M.R. D’Orsogna, J. Rudnick, Fluctuation-facilitated charge migration along DNA, *Phys. Rev. Lett.* 85 (2000) 4393–4396.
- [23] E.M. Conwell, S.V. Rakhmanova, Polarons in DNA, *Proc. Natl. Acad. Sci. U. S. A.* 97 (2000) 4556–4560.
- [24] M.A. Young, G. Ravishanker, D.L. Beveridge, A 5-nanosecond molecular dynamics trajectory for B-DNA: analysis of structure, motions, and solvation, *Biophys. J.* 73 (1997) 2313.
- [25] T. Holstein, Studies of polaron motion: Part I: the molecular-crystal model, *Ann. Phys.* 8 (1959) 325–342.
- [26] K.L. Wang, Q.H. Chen, S.L. Wan, A concise approach to the calculation of the polaron ground-state energy, *Phys. Lett. A* 185 (1994) 216–220; Y. Wang, K.L. Wang, S.L. Wan, J.L. Yang, General properties for two-dimensional polarons with non-zero momentum, *Phys. Lett. A* 220 (1996) 131–136.
- [27] D.M. Basko, E.M. Conwell, Self-trapping versus trapping: application to hole transport in DNA, *Phys. Rev. E* 65 (7) (2002) 061902.
- [28] R.S. Han, Z.J. Lin, K.L. Wang, Exact solutions for the two-site Holstein model, *Phys. Rev. B* 65 (5) (2002) 174303.